

# Dynamic of night-time equatorial F layer: equinox transition at the magnetic equator in Africa

*S. K. Tanoh<sup>1</sup>, B. J.-P. Adohi*

Laboratoire de Physique de l'atmosphère, Université de Cocody, 22 BP 582 Abidjan 22, Ivory Coast

<sup>1</sup> [serge.koua@yahoo.fr](mailto:serge.koua@yahoo.fr)

## Abstract.

We study equatorial night-time F layer behaviour from quarter-hourly ionograms at Korhogo/Ivory Coast (9.2°N, 5°W, dip lat. -2.4°) during local Spring March-April 1995, declining solar flux period, according to the magnetic activity. The height and thickness of the F-layer are found to vary intensely with time and from one day to the next. At time of the equinox transition, by the end of March, a net change of the nightly height-time variation is observed. The regime of a single height peak phase before 22 March changes to up to three main F-layer height phases after 30 March, each associated to a dominant mechanism. After the 21 April magnetic-equinox period, the height-time morphology becomes more irregular suggesting meridional wind abatement.

## 1. Introduction

Dynamic of the ionosphere is the result of physical and chemical processes such as thermospheric motions (winds, gravity waves ...), solar activity, productions and losses of ions. Most of the observations and studies were carried out on the night-time heights variations of ionosphere, generally from 18:00 to 00:00 LT, and have not concerned African region [1]; [2]. At equatorial latitudes, the prereversal enhancement of eastward zonal electric field (or post-sunset E x B pulse) causes a rising of F layer [3]; [4]; [5]. The intensity of this phenomenon depends on several factors including the season, the magnetic activity, and the phase of the solar cycle [6].

The midnight temperature maximum (MTM) is an enhancement in neutral temperature which occurs near local midnight at low latitudes [7]. The MTM initially forms at the geographic equator and propagates towards the poles. The temperature enhancement is accompanied by a pressure increase which, in turn, can result in a reversal or abatement in the meridional winds from equator to pole. This modification in the winds initiates the «midnight collapse» of the F layer which moves plasma to lower (or upper) altitudes.

We study equatorial night-time behaviour from 18:00 to 06:00. We describe March and April 1995 results from quarter-hourly IPS 42 ionograms at Korhogo/Ivory Coast. They cover the local spring transition at this near magnetic-equatorial site. Section 2 discusses the equinox transition in West Africa.

## 2. Data and method of analysis

The device set up at Korhogo /Ivory Coast is a vertical sounding IPS 42 transmitter–receiver. The aerial has 80 m width and 25 m height. The power transmitter pulse is well shaped with 2  $\mu$ s rise time and 10  $\mu$ s width, and the peak power transmitter is 5 kW. The ionosonde explores the HF frequency range [1 MHz – 22 MHz]. It records the continuous frequency sweeping echoes reflected at the ground and provides the electron-density profiles of the lower ionosphere in virtual coordinate every 15 min. At low latitude the sequences of such profiles gives a regular sampling of the F-layer evolution.

Two altitude parameters are commonly determined from the electron-density profiles. The bottom level altitude h'F is extrapolated from the low-frequency asymptotic value of the virtual height. The peak level altitude hpF is read on the ordinary trace and is taken as the virtual height for the plasma frequency. The parameters h'F and hpF are estimate every quarter hour and their plot in the 2-D coordinates system (height, time) delimitates the F-layer semi-thickness at any time and allows studying F-layer dynamics.

## 3. Time variation of the f-layer parameters around the spring equinox

### 3.1. Time dependence of the F-layer height

Figure 1 shows the typical time dependences of the F layer height registered during all the spring equinox period of March-April 1995.

The lower curve corresponds to altitude of the bottom of the layer  $h'F$  and the upper one to that of the F-layer maximum electronic density  $hpF$ . On 8-9 March (figure 1a), a quiet night ( $A_m = 6$ ) preceding a period of increasing magnetic index (Table 1), the F layer height exhibits a single phase of rise (from 18:00 UT to 20:15 UT) and descent (from 20:15 UT to 23:00 UT) of the layer. The elevation at the bottom of the layer is about 100 km. During all the rest of the night the height remains constant at about 205 km until sunrise. This is the well-known post-sunset peak [1] usually attributed to the  $E \times B$  ionosphere electric field pulse.

Figure 1b shows the example of 3-4 April, also quiet night ( $A_m = 2$ ). The variation clearly exhibits a three-phase pattern. Phase 1 is the post-sunset peak described above. Phase 2 occurs between 00:00 UT and 04:00 UT. Its peak is located at about 02:00 UT. The layer goes up from  $h'F = 215$  km to  $h'F = 255$  km. the rise and descent have average velocities of about 16m/s and 10m/s, respectively. Phase 3 is a pre-sunrise motion starting at about 04:00 UT. Most often in our experiments this phase is not entirely observed.

Figure 1c shows the example of 20-21 April, another quiet night ( $A_m = 14$ ) preceding a moderately disturbed period. The pattern is a single huge peak extended from 18:00 UT to 03:00 UT. It shows evidence of a three-time motion as follows. A post-sunset rise at about 10m/s mean apparent velocity takes the bottom of the layer from 245 km at 18:00 UT up to 310 km at 20:00 UT. Then the layer remains practically stationary until 01:00. the descent follows and takes the layer down to 230 km at 02:00 UT with a mean apparent velocity of 13m/s. the main difference between this profile and the one of 8-9 March (fig. 1a) is the plateau region between the rise and the descent in 20-21 April (Fig. 1c). The three shapes so described above will be referred as A, B and C for Fig. 1a, b, and c, respectively. In other respect, in our set of nightly patterns, few other configurations were observed. They occurred randomly and no similitude could be detected with types A, B and C. We regrouped these particular shapes in the same label. They will be referred as O (others). Figure 1d and 1e show an example type O. In 26-27 April (Fig. 1d), the F-layer rises above 400 km after 01:00 UT. The layer density is so reduced that it was not possible to detect it by ionosonde. In 27-28 April (Fig. 1e) the peak of phase 1 usually expected between 18:00 UT and 23:00 UT is inexistent.

### 3.2. Classification

Table 2 classifies the nightly patterns observed through the equinox period and gives the occurrence percentage of each type. The geographic equinox interval around 30 March shows a clear transition in occurrence of the layer types defined previously. Before 22 March, type A dominates with 20 out of 22 cases, despite the strong magnetic storm of 9 to 14 March. From 30 March to 19 April, type B dominates with 18 out of the 21 nights, then a transition to type C and / or O occurs.

On figure 2 the plot of the bottom height  $h'F$  of the F-layer, from 6 to 20 March, allows to study the night to night variation of the A-type motion. It is interesting to notice that there is not a strong dispersion of  $h'F$  values in these 15 nights.

On figure 3 we compare type B patterns. On figure 3b the peak amplitude of phase 2, the F-layer thickness and the bottom height  $h'F$  are greater than on the other night (Fig. 3a). During the night (1-2 April) the magnetic activity presents an important increase that explains the difference, table 3 providing the three-hourly night-values of the  $A_m$  index. Whatever the profile of the F-layer parameters, the magnetic activity increase during nighttime has an impact on their amplitude. However, it does not modify the variation type, except in certain case of type O. During the period 30 March-20 April, as shown in table 2, 18 nights out of 21 have a type B variation. The three nights with type O occur after a large disturbed magnetic activity (see table 3). Thus we considered that type B variation is characteristic of the transition period after the spring equinox.

### 4. Discussion

The set of results obtained over the two months investigated suggests 3 different periods.

The A-type profile until 30 March is classically explained by the  $ExB$  drift that controls the F-layer motion. Between 30 March and 20 April, the B-type variation is observed. The first phase presents like type A and can be attributed to the  $ExB$  drift. The second phase is characterized by another peak which presence is not related to the magnetic activity as it also exists on quiet nights. However the amplitude of this second peak increases with increasing magnetic activity. This suggests that other physical processes are involved. A good candidate is the MTM which cause a change in wind pattern during the equinox period [8]. During the whole year the dominant wind patterns correspond to the solstice ones with a circulation from the summer hemisphere to the winter one. The equinox period circulation lasts a few weeks after the equator solar transit as models and observations point out [8]. This circulation goes from a divergent situation, i.e from the equator to the poles in each hemisphere on day time and to a convergent one during night time, the inversion time depending on the location. In equinox condition the situation is complex due to the inversion of the meridional wind during nighttime that could explain the second peak.

Several hours after the beginning of a storm or strong magnetic activity, the ionospheric disturbance dynamo process [9] affects the wind circulation and associated dynamo electric fields at low latitudes. Its effect lasts several days. Ionospheric disturbance dynamo is a good candidate for the change from type B to type O.

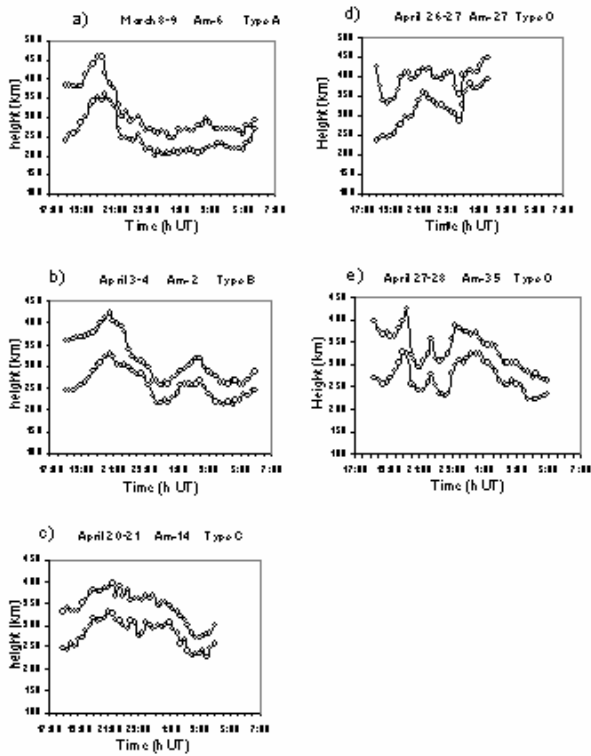


**Fig.1.** Typical height variations in kilometers at Korhogo as a function of UT time, (a) the type A showing post- sunset rise, (b) the type B with post- sunset rise plus a second height peak after midnight, (c) the abnormally wide single peak C centred near midnight, (d) and (e) O-type contour. Note that O-type contour change from one day to the next and do not show any similarity with the A, B and C-type ones.

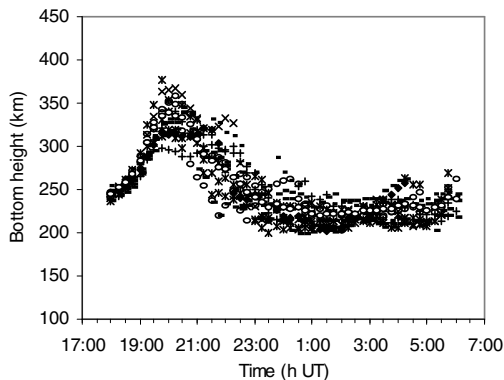


**Fig.2.** Night to night variability of the bottom height  $h'F$  of the F layer in kilometers (y-axis) as a function of UT time (x-axis), from 6 March to 20 March 1995. The profile exhibits A-type contours.

**Table 1.** Daily magnetic index Am for the period 1 March -30 April.

March	Am	March	Am	April	Am	April	Am
1	48	17	14	1	18	16	5
2	38	18	7	2	29	17	8
3	10	19	6	3	2	18	13
4	37	20	8	4	5	19	11
5	27	21	2	5	16	20	14
6	6	22	4	6	8	21	2
7	4	23	13	7	121	22	19
8	6	24	10	8	49	23	37
9	27	25	8	9	34	24	41
10	27	26	50	10	37	25	28
11	45	27	36	11	34	26	27
12	52	28	29	12	27	27	35
13	58	29	28	13	12	28	22
14	31	30	14	14	7	29	13
15	22	31	14	15	4	30	5
16	20						

**Table 2.** Classification of the F-layer profiles according to their nightly patterns for the period 1 March-30 April. Type A corresponds to a single post-sunset peak (Fig.1a), type B (Fig.1b), and type C (fig.1c). Type O correspond to undefined, odd profiles.

March	Nightly contour-types of the F-layer for the period 1 March-30 April				April				
	(A)	(B)	(C)	Other (O)		(A)	(B)	(C)	Other (O)
1_2				X	1_2			X	
2_3				X	2_3				X
3_4	X				3_4		X		
4_5	X				4_5		X		
5_6	X				5_6		X		
6_7	X				6_7		X		
7_8	X				7_8		X		
8_9	X				8_9				X
9_10	X				9_10				X
10_11	X				10_11		X		
11_12	X				11_12		X		
12_13	X				12_13		X		
13_14	X				13_14		X		
14_15	X				14_15		X		
15_16	X				15_16		X		
16_17	X				16_17		X		
17_18	X				17_18		X		
18_19	X				18_19		X		
19_20	X				19_20		X		
20_21	X				20_21				X
21_22	X				21_22				X
22_23	X				22_23				X
23_24				X	23_24				X
24_25		X			24_25			X	
25_26	X				25_26			X	
26_27				X	26_27				X
27_28	X				27_28				X
28_29	X				28_29				X
29_30	X				29_30				X
30_31		X			30_1er				X
31_1er		X							
Case total	24	3	0	4	Case total	0	16	5	9

Statistic of the observations over the whole March-April equinox period

	(A)	(B)	(C)	Other (O)
Number of observations	24	19	5	13
Occurrence (%)	39.3	31.1	8.2	21.3

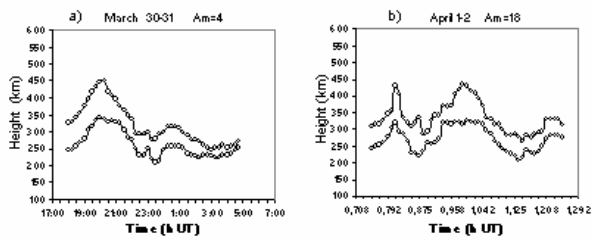


**Fig.3.** Night to night variability of the bottom height  $h'F$  and the height of maximum electronic density  $hpF$  of the F layer in kilometers (y-axis) as a function of UT time (x-axis) for 2 nights with B-type contours, (a) 30-31 March, (b) 1-2 April.

**Table 3.** Three-hourly magnetic index  $Am$ , for the night plotted in the different figures

Nights	Layer types	18h-21h	21h-24h	0h-3h	3h-6h
8-9 March	A	8	6	7	18
30-31 March	B	7	4	6	10
1-2 April	B	56	44	44	63
3-4 April	B	1	1	9	2
20-21 April	C	8	6	1	2
26-27 April	O	26	50	33	22
27-28 April	O	24	8	13	22

## 5. Conclusion

Height-time profiles of the F-layer are analysed based on quarter-hourly ionograms continuously registered at Korhogo/Ivory Coast ( $9.2^{\circ}N$ ,  $5^{\circ}W$ , dip lat.  $-2.4^{\circ}$ ) in the West African sector during the two-month March-April 1995 period.

We showed that in addition to the single rise and fall motion generally observed after sunset, others exist depending on the period. Three distinct periods were so identified.

- Before 22 March, only the single rise and fall motion associated to the post-sunset electric field enhancement occurs.
- Between 30 March and 21 April two additional motions occur after the post-sunset one. Both peaks shift along with time and their amplitude increases with increasing magnetic activity.
- After 21 April none of the two precedent profiles exists. The F-layer pattern shows either a single huge peak with a plateau region or an odd profile with no similitude with the precedents. The period around 22 March and 21 April being the equinox solar-transit period, the above changes in height-time profiles were identified as an effect of the equinox transition and the additional peaks characterized in the light of actual knowledge on this phenomenon.

## References

- [1] Fejer, B. G., Farley, D. T., Woodman, R. F., and Calderon, C.: Dependence of equatorial F region vertical drifts on season and solar cycle, *J. Geophys. Res.*, 84, 5792-5796, 1979.
- [2] Sastri, J. H., Abdu, M. A., Bastia, I. S., and Sobral, J. H. A.: Onset conditions of equatorial (range) spread F at Fortaleza, Brazil, during the June solstice, *J. Geophys. Res.*, 102(A11), 24013-24021, 1997.
- [3] Heelis, R. A., P. C. Kendal, R. J. Moffet, D. W. Windle, and H. Rishbeth, Electric coupling of the E and F regions and its effect on F region drifts and winds, *Planet. Space Sci.*, 22, 743, 1974.
- [4] Matuura, N., Electric fields from the thermospheric model, *J. Geophys. Res.*, 79, 4679, 1974.
- [5] Rishbeth, H., The F-region dynamo, *J Atmos. Terr. Phys.*, 43, 387, 1981.
- [6] Farley, D. T., Bonelli, E., Fejer, B. G., and Larsen, M. F.: The prereversal enhancement of the zonal electric field in the equatorial ionosphere, *J. Geophys. Res.*, 91, 13723- 13728, 1986.
- [7] Mayr H.G., Harris I., Spencer N.W., Hedin A.E., Wharton L.E., Potten H.S., Walker J.C.G., Carlson H.C., Tide and the midnight temperature anomaly in the thermosphere. *Geophys. Res. Lett.* 6, 447- 450, 1979.
- [8] Roble, R. G., Dickinson, R. E., and Ridley, E. C.: Seasonal and Solar cycle variations of the zonal mean circulation in the thermosphere, *J. Geophys. Res.*, 82(35), 5493-5504, 1977.
- [9] Blanc M. and Richmond, A.: The ionospheric disturbance dynamo, *J. Geophys. Res.*, 85, 1669-1686, 1980.